

Uncertainty Cost of Stochastic Producers: Metrics and Impacts on Power Grid Flexibility

Farzaneh Pourahmadi, *Student Member, IEEE*, Seyed Hamid Hosseini ^{id}, *Member, IEEE*,
Payman Dehghanian ^{id}, *Member, IEEE*, Ekundayo Shittu ^{id}, *Member, IEEE*,
and Mahmud Fotuhi-Firuzabad ^{id}, *Fellow, IEEE*

Abstract—The widespread presence of contingent generation, when coupled with the resulting volatility of the chronological net-load (i.e., the difference between stochastic generation and uncertain load) in today’s modern electricity markets, engender the significant operational risks of an uncertain sufficiency of flexible energy capacity. In this article, we address several operational flexibility concerns that originate from the increase in generation variability captured within a security-constrained unit commitment (SCUC) formulation in smart grids. To quantitatively assess the power grid operational flexibility capacity, we first introduce two reference operation strategies based on a two-stage robust SCUC, one through a fixed and the other via an adjustable uncertainty set, for which the state-of-the-art techniques may not be always feasible, efficient, and practical. To address these concerns and to account for the effects of the uncertainty cost resulting from dispatch limitations of flexible resources, a new framework centered on the adjustable penetration of stochastic generation is proposed. Our hypothesis is that if the SCUC is scheduled with an appropriate dispatch level of stochastic generation, the system uncertainty cost will decrease, and subsequently, the system’s ability to accommodate additional uncertainty will improve. Numerical simulations on a modified IEEE 73-bus test system verify the efficiency of the suggested assessment techniques.

Index Terms—Adjustable penetration, operational flexibility, optimal uncertainty set, stochastic generation, wind power.

NOMENCLATURE

A. Indices

i Index for generating units.
 k Index for wind farms.

Manuscript received February 22, 2019; revised October 22, 2019; accepted January 21, 2020. Date of publication February 25, 2020; date of current version February 21, 2022. This work was partially supported by the National Science Foundation under Award 1847077. Review of this manuscript was arranged by Department Editor T. Hong. (*Corresponding author: Farzaneh Pourahmadi.*)

F. Pourahmadi, S. H. Hosseini, and M. Fotuhi-Firuzabad are with the Center of Excellence in Power System Management, Department of Electrical Engineering, Sharif University of Technology, Tehran 11365-11155, Iran (e-mail: pourahmadi_f@ee.sharif.edu; hosseini@sharif.edu; fotuhi@sharif.edu).

P. Dehghanian is with the Department of Electrical and Computer Engineering, George Washington University, Washington, DC 20052 USA (e-mail: payman@gwu.edu).

E. Shittu is with the Department of Engineering Management and Systems Engineering, George Washington University, Washington, DC 20052 USA (e-mail: eshittu@gwu.edu).

Color versions of one or more of the figures in this article are available online at <http://ieeexplore.ieee.org>.

Digital Object Identifier 10.1109/TEM.2020.2970729

l Index for transmission lines.
 m Index for load points.
 t Index for time periods.

B. Variables

b_{kt} Binary variables indicating the worst variation of wind farm k in time period t .
 u_{it}^b Binary variable indicating whether generating unit i starts up in time period t in the base-case scenario.
 v_{it}^b Binary variable indicating whether generating unit i shuts down in time period t in the base-case scenario.
 x_{it}^b Binary variable indicating on/off status of generating unit i in time period t in the base-case scenario.
 p_{it}^b, p_{it}^u Production of generating unit i in time period t in the base-case scenario and in response to uncertainties, respectively.
 q_{kt} Degeneration coefficient of wind farm k in time period t .
 w_{kt} Power output of wind farm k in time period t .
 w_{kt}^{LB}, w_{kt}^{UB} Lower and upper bounds for allowable wind generation interval of wind farm k in time period t , respectively.
 s_{kt}, l_{mt} Curtailment of load m and generation of wind farm k in time period t .
 ω_{kt} Dispatched power of wind farm k in time period t in ex-ante manner.

C. Parameters

$\overline{w_{kt}}$ Forecasted output of wind farm k in time period t .
 $w_{kt}^{\min}, w_{kt}^{\max}$ Lower and upper bounds of the predicted wind generation interval of wind farm k in time period t , respectively.
 $H_l^{[.]}$ Generation shift distribution factor of generating unit i , wind farm k , and load m corresponding to transmission line l .
 F_l^{\max} Maximum capacity of transmission line l .
 γ_l Short-term rating factor of transmission line l .
 d_{mt} Demand at load point m in time period t .
 c_i^u, c_i^d Start-up and shut-down costs of generating unit i , respectively.

c_i^p, c_i^r	Production and reserve cost of generating unit i , respectively.
c_k^w, c_m^l	Cost coefficients of spillage for wind farm k and load shedding of load point m , respectively.
sc_t, lc_t	Cost coefficients of wind spillage and load shedding in time period t , respectively.
P_i^{\min}, P_i^{\max}	Minimum and Maximum output power of generating unit i in time period t , respectively.
$R_i^{\text{UP}}, R_i^{\text{DN}}$	Up/down corrective action limits of generating unit i , respectively.
RD_i, RU_i	Downward and upward ramping capability of generating unit i , respectively.
T	Number of time periods.

I. INTRODUCTION

THE deployment of renewable energy sources (RESs) has been observed to be significantly on the rise worldwide. This development is fueled by the strengthening and expansion of policies aimed at the reduction of greenhouse gas emissions. These policies are expected to ensure and even expedite a sustainable growth in the penetration of RESs in the electric industry. To quantify this, 37 states in the U.S. have implemented renewable portfolio standards. These standards mandate electricity producers or utilities to generate between 10% and 33% of their outputs from a renewable resource. Likewise, the European Union has legislated policies to achieve the targets of 20% renewable energy penetration by 2020 [1], [2]. It is well established that these renewable resources (mainly wind and solar) are highly intermittent leading to supply variabilities. This variability in the net load—forecasted electricity demand minus stochastic generation—will contribute to new operational challenges in bulk power grids, such as operation limit violations, frequent startups and shutdowns of dispatchable generating units, reduction in available lead time, and increased ramping and reserve requirements [3]. These intensified operational challenges can be ameliorated through improvements in system flexibility.

Advanced and effective flexibility metrics, if derived meticulously, can assess the system's ability in deploying its resources to respond to a range of uncertain conditions. It can, in turn, help the power system planners to decide on generation regulatory policies to better tackle the operational flexibility challenges in modern power grids. The notion of flexibility and its metrics requires the crucial aspects of system operation to be taken into account [4]. Assessing the net-load stochasticity and the corresponding flexibility measurements can be modeled either explicitly or implicitly. In the explicit model, the system net-load is quantified such that the flexibility requirements are embedded in the optimization models through a reserve constraint [5]–[7]. In an attempt to thoroughly address the intrahourly spectrum of flexibility requirements, the flexibility envelope in [8], the flying brick in [9], and the probability box in [10] were suggested, among the others, which could capture both the reserve ramping and capacity requirements. In the implicit model, however, the net-load uncertainties are integrated into the optimization model to be solved via stochastic or robust

optimization (RO) techniques, where reserve requirements are accounted for through satisfaction of the power balance constraint under uncertain conditions [11], [12]. In such stochastic models, an economic strategy over a set of generated scenarios of uncertain parameters, or the worst-case scenario in the RO models, is the outcome [13]–[15]. With a few number of scenarios, RO models are computationally more tractable and immunized against all uncertainty realizations [16]–[18]. Several two-stage RO frameworks have been proposed in [19]–[24] to characterize and quantify the system flexibility in the worst possible scenario within the uncertainty set.

A system flexibility metric in the operational time frame can be achieved based on the RO or stochastic programming techniques. In the RO-based assessments, the system flexibility is characterized irrespective of the probability distribution of uncertainties while maintaining the stochastic nature of renewable resources. In such models, the metrics are calculated based on the set boundaries of uncertainties. In other words, these metrics answer the question of “*how much capacity should a system have to cope with the uncertainties?*” The RO-driven deterministic metrics of system flexibility, in terms of do-not-exceed limits, are formulated in [21] and [22] to assess the largest uncertainty interval that a power system can accommodate. In probabilistic assessments, however, the system's ability to satisfy a predetermined reliability criterion is probabilistically measured in [19] through a lack of ramp probability index in which sufficient ramp delivery in a real-time electricity market is ensured. In [20], the probabilistic nature of contingencies and deterministic nature of wind generation are modeled to recognize the insufficient flexibility.

As RO-based metrics are more intuitive and preferable for the decision makers in system problems where the exact distribution of uncertainties is unknown, our proposed approach to tractably quantify the power grid flexibility is centered on the RO-based metrics. The system operational flexibility should be represented in the unit commitment (UC) problem that captures the chronological characteristics of the net-load. Hence, discrete commitment decisions and temporal load and renewable variations can be modeled in the UC time scale, thereby enabling capturing the key operational flexibility requirements, e.g., binary commitment decisions, minimum up/down time, and ramping constraints. An approach to assess the grid operational flexibility irrespective of the probability distribution of the uncertainties in the UC time scale is to frame the decision variables based on the boundaries of the uncertainty set in the security-constrained unit commitment (SCUC) formulation. In this case, the maximum uncertainty interval that a system can accommodate can be quantified such that the worst security violation in response to uncertainties would be zero [23]. In [23] and [24], a two-stage robust SCUC with variable uncertainty set boundaries—exploited as the dispatch signals for wind farms—is formulated for the operational flexibility assessment where the risk of wind curtailment and load shedding are cooptimized with the generation dispatch cost.

While a number of metrics have been proposed to account for the different aspects of grid flexibility, the focus in the state-of-the-art research has been primarily on the existence of feasible

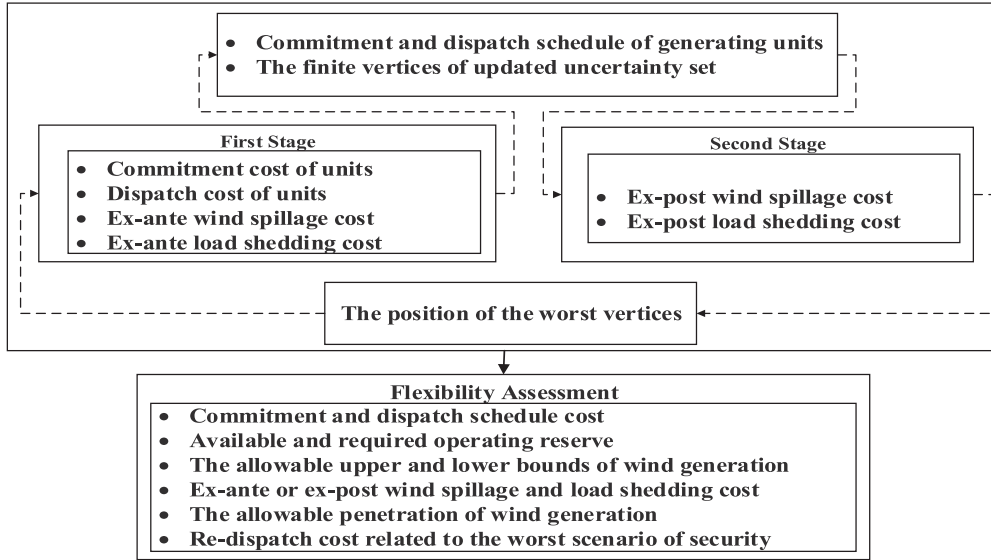


Fig. 1. General procedure for operational flexibility assessment based on the two-stage RO model and the vertex position method.

operation schedules, ignoring the impacts and contributions of redispatch costs, wind spillage costs, and load shedding costs collectively referred to as the *uncertainty cost*. In this article, we propose a new and efficient operating strategy to assess the grid operational flexibility capacity that captures the system uncertainties via dynamic adjustment of the stochastic producers' generation portfolio. Contrary to the traditional mindset on dispatching the stochastic producers always at the mean production, our hypothesis is to adjust their penetration dynamically with respect to the system's flexible capacity to yield an economically attractive solution. The main contributions of this article are summarized as follows.

- 1) *Modeling Advancements*: The proposed model provides a mathematical foundation that ensures the optimality robustness of redispatch actions against all deviations from the base-case scenario and enables the quantitative assessment of the flexible capacity availability and sufficiency along with the maximum deviation from the optimal economic points during uncertainty scenarios.
- 2) *Operational Advancements*: A novel and efficient operating strategy based on a two-stage RO formulation is proposed that can best handle the uncertainty and variability of the net-load in SCUC. Through an adjustable generation portfolio of stochastic producers, the system is promised to be immunized against the risk of security violations.

The rest of this article is structured as follows. In Section II, we introduce two existing flexibility assessment models based on the SCUC formulations. The proposed model centered on adjustable stochastic production considering the robustness of redispatch scenarios is presented in Section III. The solution technique to solve the proposed optimization model is introduced and discussed in detail in Section IV. Numerical simulations are conducted in Section V and, finally, Section VI concludes the article.

II. FLEXIBILITY ASSESSMENT IN SCUC: STATE-OF-THE-ART

In this section, we introduce state-of-the-art two-stage RO models based on the vertex position approach that enable an independent system operator to assess the power grid's flexibility capacity to economically respond to adjustable [23], [24] and fixed uncertainty sets corresponding to stochastic generation [16], [17]. The general procedure to assess the operational flexibility based on the two-stage robust SCUC model and the vertex position approach is demonstrated in Fig. 1. In the first stage, the production of stochastic producers is optimally adjusted, followed by a second stage in which the recourse (uncertainty) cost—including the redispatch, wind spillage, and load shedding costs—is minimized. In the following, assessment techniques of the state-of-the-art strategies are explained in detail.

A. SCUC Model With Adjustable Uncertainty Interval

In the first assessment technique, the maximum uncertainty region that a system can handle without any security violation is found. In other words, the uncertainty set is considered as a decision variable to realize an optimal uncertainty set while minimizing the system operation cost. In this strategy, the optimal uncertainty interval is considered as a flexibility metric that can be assessed through the following formulations:

$$\min_{P^b, X^b, w^{UB}, w^{LB}} \sum_t \sum_i c_i^p p_{it}^b + c_i^u u_{it}^b + c_i^d v_{it}^b + \sum_t \sum_k s c_t (w_{kt}^{\max} - w_{kt}^{UB}) + l c_t (w_{kt}^{LB} - w_{kt}^{\min}) \quad (1)$$

$$\text{s.t.} \quad -x_{i(t-1)}^b + x_{it}^b - x_{i\tau}^b \leq 0 \quad \forall i \forall t \forall \tau$$

$$\in \{t, \dots, MU_i + t - 1\} \quad (2a)$$

$$x_{i(t-1)}^b - x_{it}^b + x_{i\tau}^b \leq 1 \quad \forall i \forall t \forall \tau \in \{t, \dots, MD_i + t - 1\} \quad (2b)$$

$$-x_{i(t-1)}^b + x_{it}^b - u_{it}^b \leq 0 \quad \forall i \forall t \quad (2c)$$

$$x_{i(t-1)}^b - x_{it}^b - v_{it}^b \leq 0 \quad \forall i \forall t \quad (2d)$$

$$x_{it}^b, u_{it}^b, v_{it}^b \in \{0, 1\}, \quad x_{i0}^b = 0 \quad \forall i \forall t \quad (2e)$$

$$P_i^{\min} x_{it}^b \leq p_{it}^b \leq P_i^{\max} x_{it}^b \quad \forall i \forall t \quad (2f)$$

$$p_{it}^b - p_{i(t-1)}^b \leq x_{i(t-1)}^b \text{RU}_i + (1 - x_{i(t-1)}^b) P_i^{\min} \quad \forall i \forall t \quad (2g)$$

$$p_{i(t-1)}^b - p_{it}^b \leq x_{it}^b \text{RD}_i + (1 - x_{it}^b) P_i^{\min} \quad \forall i \forall t \quad (2h)$$

$$\begin{aligned} -F_l^{\max} &\leq \sum_{i \in \Lambda} H_l^i p_{it}^b + \sum_{k \in \kappa} H_l^k \omega_{kt} - \sum_{m \in M} H_l^m d_{mt} \\ &\leq F_l^{\max} \quad \forall l \forall t \end{aligned} \quad (2i)$$

$$\sum_i p_{it}^b + \sum_k \omega_{kt} = \sum_m d_{mt} \quad \forall t \quad (2j)$$

$$0 \leq \omega_{kt} \leq \bar{w}_{kt} \quad (2k)$$

$$\bar{w}_{kt} \leq w_{kt}^{\text{UB}} \leq w_{kt}^{\max} \quad (2l)$$

$$w_{kt}^{\min} \leq w_{kt}^{\text{LB}} \leq \bar{w}_{kt} \quad (2m)$$

$$P_{ib}^{\min} x_{it}^b \leq p_{it}^u \leq P_{ib}^{\max} x_{it}^b \quad [\alpha_{it}^L, \alpha_{it}^U] \quad \forall i \forall t \quad (3a)$$

$$p_{it}^u - p_{it}^b \leq R_i^{\text{UP}} x_{it}^b \quad [\zeta_{it}] \quad \forall i \forall t \quad (3b)$$

$$p_{it}^b - p_{it}^u \leq R_i^{\text{DN}} x_{it}^b \quad [\xi_{it}] \quad \forall i \forall t \quad (3c)$$

$$\begin{aligned} -F_l^{\max} &\leq \sum_{i \in \Lambda} H_l^i p_{it}^u + \sum_{k \in \kappa} H_l^k \omega_{kt} \\ &- \sum_{m \in M} H_l^m d_{mt} \leq F_l^{\max} \quad \forall l \forall t \forall w_{kt} \in [w_{kt}^{\text{LB}}, w_{kt}^{\text{UB}}] \end{aligned} \quad (3d)$$

$$\sum_i p_{it}^u + \sum_k \omega_{kt} = \sum_m d_{mt} \quad \forall t \forall w_{kt} \in [w_{kt}^{\text{LB}}, w_{kt}^{\text{UB}}]. \quad (3e)$$

The objective function (1) minimizes the base-case operation cost as well as the wind spillage and load shedding costs corresponding to the shrinking uncertainty set. The wind spillage cost is considered if the wind power exceeds an upper bound. Otherwise, load shedding cost is quantified. While a minimized operation cost in the base-case condition leads to a narrower uncertainty set, consideration of the wind spillage and load shedding costs enlarges the set of wind production uncertainty. A balance factor is adapted through the suggested penalty coefficients sc_t and lc_t . The optimal uncertainty set solution represents a secure accommodation of wind power and can then be used as the ex-ante dispatch signals for wind farms. Constraints (2a) and (2b) enforces the generators' minimum ON/OFF time; the start-up and shut-down status of generators is presented in (2c)–(2e); the capacity limits of generators are ensured in (2f); the ramping constraints for generating units are enforced in (2g) and (2h); transmission line capacity constraints are presented in (2i); the system power balance is ensured in (2j); and the generation limits of wind farms are set in (2k). At this first stage, the decision variables w^{UB} and w^{LB} are determined. Constraints (2l) and (2m) reflect the limitations on the boundaries for these two variables. The uncertainty characterization is accomplished

in the second stage presented in (3a)–(3e). Constraint (3a) limits the generation capacity and constraints (3b) and (3c) represents the ramping capability of the generating units. Constraints (3d) and (3e) ensure the power balance and the limits on transmission line power flow under uncertain conditions. This second-stage formulation will lead to a secure (i.e., feasible) schedule for all wind power realizations in the variable uncertainty set. As one can see, the load shedding and wind spillage actions due to a shrunk feasible uncertainty set are implemented in the first stage in an ex-ante manner such that the power balance and transmission line limitations would be satisfied for all uncertainty realizations.

B. SCUC Model With Fixed Uncertainty Interval

An adjustable uncertainty set may not always be feasible or efficient, owing to the fact that imposing a lower boundary of the optimal uncertainty set for wind generation as an operation signal to wind farms may not be practical. Moreover, assessment of the load shedding costs (the coefficient lc_t) in the first stage may be challenging due to the unknown list of load priorities. Hence, the second stage of the RO model is modified to have the worst load shedding and wind spillage costs optimized and assessed in an ex-post manner when dealing with the nonadjustable uncertainty sets. The objective function in the first stage would, hence, neglect the terms related to the shrunk uncertainty set. Contrary to the adjustable uncertainty set strategies, the worst security violation characterized in the second stage would have a minimum nonzero value considered as a flexibility metric.

III. MATHEMATICAL FORMULATIONS FOR ADJUSTABLE STOCHASTIC PRODUCTION

In some particular circumstances, the state-of-the-art adjustable and/or fixed uncertainty set techniques presented in Section II may not be feasible, efficient, or practical. The former technique based on the adjustable uncertainty set utilizes the uncertainty set boundaries as the dispatch signals for the wind farms. For any wind generation (uncertainty realization) out of a characterized uncertainty set, certain wind spillage or load shedding costs may occur that are not accounted for in the second-stage optimization; hence, the load priorities in load shedding decisions cannot be modeled. The latter utilizes the fixed uncertainty set principles where the worst load shedding and wind spillage costs are optimized in an ex-post manner, resulting in an expensive solution. Different and complementary to the state-of-the-art techniques, this article proposes a new two-stage RO formulation to evaluate the operational flexibility capacity of power grids through the effective adjustments of stochastic productions. In the first stage, the production of stochastic producers is optimally adjusted, followed by a second stage in which the recourse (uncertainty) cost—including the redispatch, wind spillage, and load shedding costs—is minimized. Traditionally, wind farms are dispatched in their expected production in the base-case scenario; we further relax this constraint where the uncertainty interval is managed by adjusting the penetration level of stochastic producers. In the systems with less penetration of stochastic producers, the variability and

stochasticity in the net-load will decrease consequently and the decrease in the production of stochastic producers will help the system security. Without the loss of generality, it is assumed in this article that the wind farms are the only source of grid stochastic production. Therefore, the following robust SCUC with an adjustable penetration rate of wind farms is suggested to immunize the system against security violations in the face of uncertainties

$$\begin{aligned} & \min_{P^b, X^b, P^u, W^{UB}, W^{LB}} \sum_t \sum_i c_i^p p_{it}^b + c_i^u u_{it}^b + c_i^d v_{it}^b \\ & + \sum_t \sum_k s_{kt} ((1 - q_{kt}) \bar{w}_{kt}) \\ & + \max_{W \in [W^{LB}, W^{UB}]} \min_{p^u} \sum_t \sum_i c_i^r p_{it}^u \end{aligned} \quad (4)$$

s.t. (2a)–(2h), (3a)–(3e)

$$\begin{aligned} -F_l^{\max} & \leq \sum_{i \in \Lambda} H_l^i p_{it}^b + \sum_{k \in \kappa} H_l^k q_{kt} \bar{w}_{kt} \\ & - \sum_{m \in M} H_l^m d_{mt} \leq F_l^{\max} \quad \forall l \quad \forall t \end{aligned} \quad (5a)$$

$$\sum_i p_{it}^b + \sum_k q_{kt} \bar{w}_{kt} = \sum_m d_{mt} \quad \forall t \quad (5b)$$

$$w_{kt}^{UB} = q_{kt} (w_{kt}^{\max} - \bar{w}_{kt}) + q_{kt} \bar{w}_{kt} \quad \forall k \quad \forall t \quad (5c)$$

$$w_{kt}^{LB} = q_{kt} \bar{w}_{kt} - q_{kt} (\bar{w}_{kt} - w_{kt}^{\min}) \quad \forall k \quad \forall t \quad (5d)$$

$$0 \leq q_{kt} \leq 1 \quad \forall k \quad \forall t. \quad (5e)$$

The objective function in (4) minimizes the base-case system operation cost and that corresponding to the production adjustment of wind farms along with the worst redispatch costs under uncertainty scenarios. Different from the state-of-art models, the robustness of redispatch actions against all uncertainty realizations is also enforced in (4). Constraints (5a) and (5b) represent the power balance and transmission limits in the base-case scenario with respect to the adjustable production of wind farms. In the proposed model, the original objective function (1) and constraints (2i)–(2l) are replaced with objective function (4) and constraints (5a)–(5e), respectively. Coefficient q_{kt} adjusts the penetration of wind farm k in time period t . By adjusting q_{kt} , in addition to the dispatched production of wind farms, the imposed uncertainty interval to the system is also adjusted. Enforced in (5e), q_{kt} varies between one and zero. For the sake of simplicity, the relationship between the wind generation penetration and its imposed uncertainty to the system is considered linear as indicated in (5c) and (5d).

IV. PROPOSED SOLUTION METHODOLOGY

In this section, two algorithms are suggested to solve the proposed optimization model. The key challenge in solving the proposed two-stage RO model lies in the second-stage (3a)–(3e) where the number of constraints is extremely large due to the arbitrary selection of w_{kt} . The benders decomposition (BD) and column and constraint generation (C&CG) methods can be

employed to replace the uncertainty set with the corresponding finite vertices. This decomposes the original problem (2a)–(2h), (3), (4), (5) into a master problem for the base-case condition and security-check subproblems for the vertices. To investigate the feasibility of (3d)–(3e) for all w_{kt} values in the uncertainty set, the following security-check subproblem (6), (7) is proposed. The non-negative slack variables s_{kt} and l_{mt} , defined as wind spillage and load shedding, are applied to evaluate the infeasibility degree of (3d)–(3e). Constraint (7a) describes the uncertainty set for w_{kt} and (7b) ensures that the slack variables are non-negative. Constraints (7c) and (7d) represent the relaxed network power flow and power balance limits.

$$\max_{w_{k,t}} \min \sum_t \sum_i c_i^r p_{it}^u + \sum_t \sum_k c_k^w s_{kt} + \sum_t \sum_m c_m^l l_{mt} \quad (6)$$

s.t. (3a)–(3c)

$$w_{kt}^{LB} \leq w_{kt} \leq w_{kt}^{UB} \quad (7a)$$

$$l_{mt} \geq 0, \quad s_{kt} \geq 0 \quad (7b)$$

$$\begin{aligned} -F_l^{\max} & \leq \sum_{i \in \Lambda} H_l^i p_{it}^u + \sum_{k \in \kappa} H_l^k w_{kt} - \sum_{k \in \kappa} H_l^k s_{kt} \\ & - \sum_{m \in M} H_l^m d_{mt} + \sum_{m \in M} H_l^m l_{mt} \leq F_l^{\max} [\mu_{lt}^L, \mu_{lt}^U] \quad \forall l \quad \forall t \end{aligned} \quad (7c)$$

$$\sum_i p_{it}^u + \sum_k w_{kt} + \sum_m l_{mt} - \sum_k s_{kt} = \sum_m d_{mt} [\lambda_t] \quad \forall t. \quad (7d)$$

A. Solution Methodology for Feasibility Check

In order to reduce the bilevel equations (3a)–(3c), (6), (7) into a monolithic one, the duality theory is applied here. Considering w_{kt} as a variable, its optimal solution is at the extreme points of the uncertainty set. Therefore, the bilinear problem can be linearized through the application of the big-M approach that yields to a mixed-integer problem (MIP) as formulated in the following:

$$\begin{aligned} Q & = \max \sum_t \sum_i \left[\alpha_{it}^{L(r)} P_{ib}^{\min} x_{it}^{b*} - \alpha_{it}^{U(r)} P_{ib}^{\max} x_{it}^{b*} \right] \\ & - \sum_t \sum_i \zeta_{it}^{(r)} (p_{it}^{b*} + R_i^{UP} x_{it}^{b*}) \\ & - \sum_t \sum_{i \in \Lambda} \xi_{it}^{(r)} (R_i^{DN} x_{it}^{b*} - p_{it}^{b*}) - \sum_t \lambda_t^{(r)} d_t^{\text{total}} \\ & + \sum_t \sum_l \left[\left(\mu_{lt}^{L(r)} - \mu_{lt}^{U(r)} \right) \sum_{m \in M} H_l^m d_{mt} \right] \\ & - \sum_t \sum_l \left[F_l^{\max} \left(\mu_{lt}^{L(r)} + \mu_{lt}^{U(r)} \right) \right] + \sum_t \sum_k \\ & \times \left[\sum_l \left[\left(\mu_{lt}^{L(r)} - \mu_{lt}^{U(r)} \right) H_l^k + \lambda_t^{(r)} \right] w_{kt}^{LB*} + \zeta_{kt}^{(r)} w_{kt}^{UB*} \right] \end{aligned} \quad (8)$$

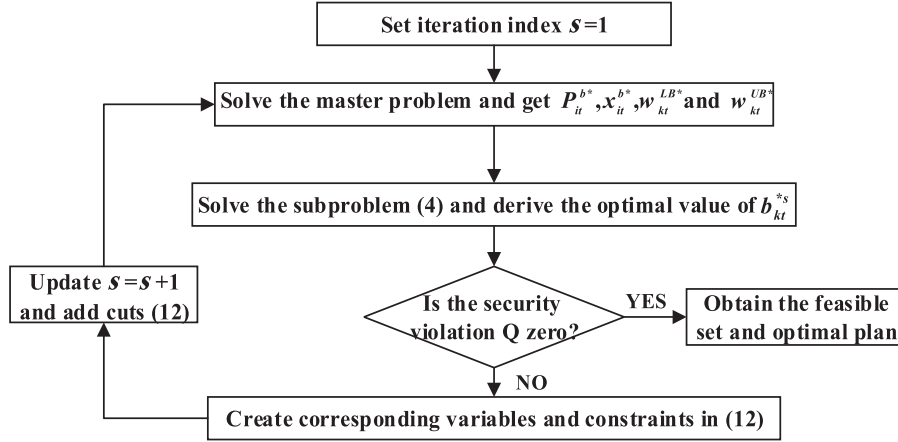


Fig. 2. Flowchart of the C&CG procedure.

s.t.

$$-M_{\text{big}} b_{kt} \leq \sum_l \left(\mu_{lt}^{L(r)} - \mu_{lt}^{U(r)} \right) H_l^k + \lambda_t^{(r)} - \zeta_{kt}^{(r)} \leq 0 \quad \forall k \forall t \quad (9a)$$

$$0 \leq \zeta_{kt}^{(r)} \leq M_{\text{big}}(1 - b_{kt}) \quad \forall k \forall t \quad (9b)$$

$$-\alpha_{it}^{U(r)} + \alpha_{it}^{L(r)} - \zeta_{it}^{(r)} + \xi_{it}^{(r)} - \lambda_t^{(r)} + \sum_{l \in \Omega} \mu_{lt}^{U(r)} H_l^i - \sum_{l \in \Omega} \mu_{lt}^{L(r)} H_l^i \leq c_i^r \quad \forall i \forall t \quad (9c)$$

$$-\lambda_t^{(r)} + \sum_{l \in \Omega} \mu_{lt}^{U(r)} H_l^m - \sum_{l \in \Omega} \mu_{lt}^{L(r)} H_l^m \leq c_m^l \quad \forall m \forall t \quad (9d)$$

$$\lambda_t^{(r)} - \sum_{l \in \Omega} \mu_{lt}^{U(r)} H_l^n + \sum_{l \in \Omega} \mu_{lt}^{L(r)} H_l^k \leq c_k^w \quad \forall k \forall t. \quad (9e)$$

Auxiliary constraints (9a) and (9b) are generated during the linearization process using the big-M method, where M_{big} is sufficiently large. With the auxiliary constraints, we will have

$$\zeta_{kt}^{(r)} = \begin{cases} 0 & \sum_l [(\mu_{lt}^{L(r)} - \mu_{lt}^{U(r)}) H_l^k + \lambda_t^{(r)}] > 0 \\ > 0 & \sum_l [(\mu_{lt}^{L(r)} - \mu_{lt}^{U(r)}) H_l^k + \lambda_t^{(r)}] \leq 0 \end{cases} \quad (10)$$

In case $\zeta_{kt}^{(r)}$ is positive, the optimal value for w_{kt} would be w_{kt}^{UB} ; otherwise, it would be w_{kt}^{LB} . Different from the conventional decomposition methods, where the exact values of the vertices are added to the first stage, here only the position of effective vertices (b_{kt}) is fed back, while continuous variables w_{kt}^{UB} and w_{kt}^{LB} are optimized with the base-case plan. In the following, two algorithms based on the C&CG and BD methods will be discussed to demonstrate how the vertices can be embedded in the master problem.

B. C&CG Method

Through the C&CG method, the proposed model is decomposed into the master problem (2a)–(2h), (5), (11), (12) and the

subproblem (8), (9). The master problem consists of the objective function (11) with (2a)–(2h), (5) and the embedded cuts obtained in (12). The solution procedure based on the C&CG method is summarized in Fig. 2. The master problem is solved to obtain the optimal solutions $P_{it}^b, x_{it}^b, w_{kt}^{\text{LB}}$, and w_{kt}^{UB} , which are passed on to the security subproblem. At each iteration (s), the MIP subproblem (8), (9) is solved, the optimal value of b_{kt}^s is obtained, and the corresponding variables and constraints are added to the master problem. The iterative procedure stops when the master solutions are obtained with no security violations.

$$\min_{P^b, X^b, P^u, W^{\text{UB}}, W^{\text{LB}}} \sum_t \sum_i c_i p_{it}^b + s_i^u u_{it}^b + s_i^d v_{it}^b + \sum_t \sum_k s c_k ((1 - q_{kt}) \bar{w}_{kt}) \quad (11)$$

$$P_{ib}^{\min} x_{it}^b \leq p_{it}^{uj} \leq P_{ib}^{\max} x_{it}^b \quad \forall i \forall t \forall j \leq s \quad (12a)$$

$$p_{it}^{uj} - p_{it}^b \leq R_i^{\text{UP}} x_{it}^b \quad \forall i \forall t \forall j \leq s \quad (12b)$$

$$p_{it}^b - p_{it}^{uj} \leq R_i^{\text{DN}} x_{it}^b \quad \forall i \forall t \forall j \leq s \quad (12c)$$

$$-F_l^{\max} \leq \sum_{i \in \Lambda} H_l^i p_{it}^{uj} + \sum_{k \in \kappa} H_l^k \left(b_{kt}^{*j} w_{kt}^{\text{LB}} + (1 - b_{kt}^{*j}) w_{kt}^{\text{UB}} \right) - \sum_{m \in M} H_l^m d_{mt} \leq F_l^{\max} \quad \forall l \forall t \forall j \leq s \quad (12d)$$

$$\sum_i p_{it}^{uj} + \sum_k b_{kt}^{*j} w_{kt}^{\text{LB}} + (1 - b_{kt}^{*j}) w_{kt}^{\text{UB}} = \sum_m d_{mt} \quad \forall t \forall j \leq s. \quad (12e)$$

C. Modified BD Method

In this section, a novel decomposition algorithm based on the L-shaped technique is proposed to be utilized in order to accelerate the solution procedure of the BD method. The suggested modified BD algorithm performs an order of magnitude faster than the conventional BD algorithms. In the conventional BD

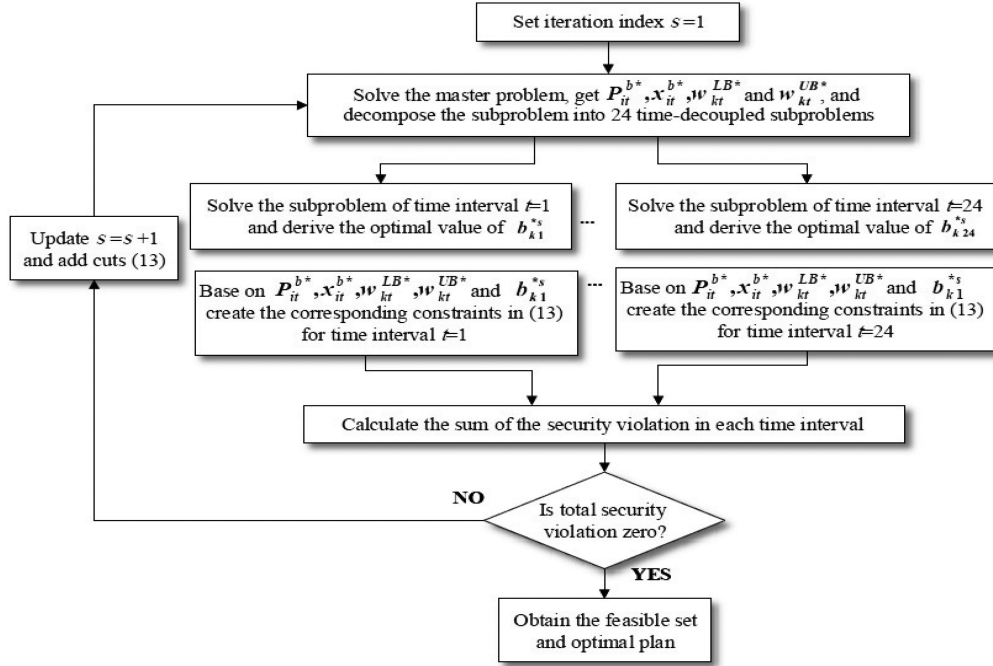


Fig. 3. Flowchart of the proposed modified BD solution method.

algorithms, one cut corresponding to the subproblem solution is embedded at each iteration to the master problem. The main idea of the L-shaped technique is to accelerate the BD algorithm performance by increasing the number of cuts added to the master problem at each iteration. Since the constraints in the optimization problem (3a)–(3c), (7) are time-decoupled, the subproblem (8), (9) is proposed to be decomposed into the smaller time-decoupled subproblems for individual time intervals, and then to be solved separately. Therefore, at each iteration and for each smaller subproblem, the corresponding constraint in (13) is generated and all 24 cuts corresponding to the 24 h are simultaneously embedded to the master problem. The procedure proposed for the modified BD algorithm is presented in Fig. 3.

$$\begin{aligned}
 & Q_t^j - \sum_k (w_{kt}^{LB} - w_{kt}^{LB*j}) \left(-\lambda_t^j + \sum_l H_l^k (\mu_{lt}^{Uj} - \mu_{lt}^{Lj}) \right) l_{kt}^{*j} \\
 & - \sum_k (w_{kt}^{UB} - w_{kt}^{UB*j}) \left(-\lambda_t^j + \sum_l H_l^k (\mu_{lt}^{Uj} - \mu_{lt}^{Lj}) \right) \\
 & \times (1 - b_{kt}^{*j}) - \sum_i (x_{it}^b - x_{it}^{b*j}) (P_{ib}^{\max} \alpha_{it}^{Uj} - P_{ib}^{\min} \alpha_{it}^{Lj}) \\
 & + R_i^{\text{UP}} \zeta_{it}^j + R_i^{\text{DN}} \xi_{it}^j - \sum_i (P_{it}^b - P_{it}^{b*j}) (\alpha_{it}^{Uj} - \alpha_{it}^{Lj}) \\
 & \leq 0 \quad \forall t = 1, \dots, 24 \quad \forall j \leq s. \quad (13)
 \end{aligned}$$

V. NUMERICAL CASE STUDY

In order to demonstrate the feasibility and effectiveness of the proposed frameworks for the quantitative assessment of power

system flexibility, numerical simulations are conducted on the modified IEEE RTS-96 test system. This test system consists of 73 buses (substations), 96 generating units, 51 load points, and 120 transmission lines [25]. The generator data and wind farm parameters are borrowed from the article presented in [26]. The forecasted uncertainty set for wind power follows $\alpha \overline{w_{kt}} \leq w_{kt} \leq \beta \overline{w_{kt}}$, where α and β are set to 0.8 and 1.2, respectively. The proposed models are solved using CPLEX 12.1 solver.

A. Adjustable Uncertainty Interval With Operating Reserve

With the forecasted uncertainty set of wind generation (20% variations) as the input, the proposed RO model is applied to characterize the largest uncertainty interval that the system can accommodate. The penalty factors corresponding to the load curtailment and wind power spillage in an ex-ante manner (due to a shrunk uncertainty set) are set at 1000\$/MWh and 100\$/MWh, respectively. Two approaches, C&CG and the modified BD, are employed to solve the proposed RO model.

Fig. 4 depicts the upper bounds of the *optimal* and *forecasted* uncertainty sets. Due to the high penalty values l_{ck} , the *optimal* and the *forecasted* lower bounds of the uncertainty set are equal. However, the *optimal* upper bound is lower than the *forecasted* one at hours 17, 22, and 23, indicating that the system lacks sufficient capacity to respond to the forecasted uncertainty set in these hours. This is primarily due to the fact that the net-load at these hours is observed negative, resulting in the lower ability of generating units to provide the downward operating reserve. Thus, the system's ability to accommodate any wind power realizations beyond the expected value has been reduced in these hours. It can also be seen in Fig. 5 that the optimal uncertainty sets (required reserve) characterized through the two approaches are very similar, except at

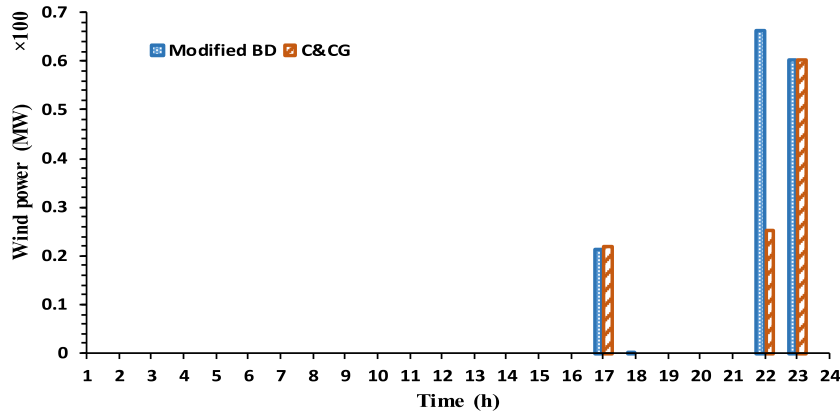


Fig. 4. Performance comparison of the C&CG and modified BD: Upper bounds of the *optimal* and the *forecasted* wind power uncertainty sets.

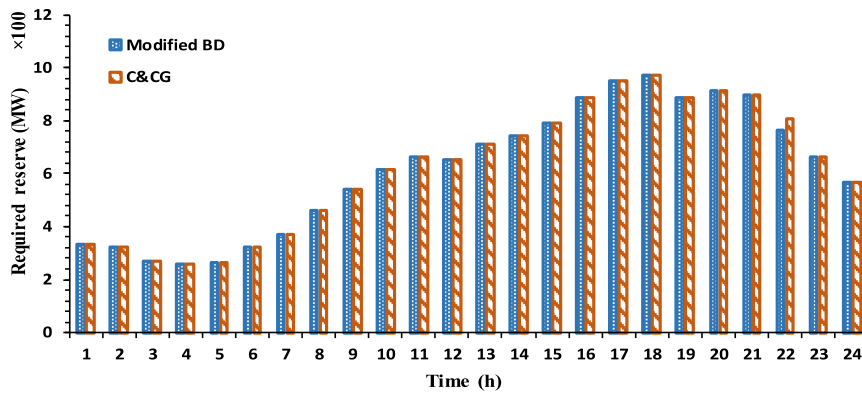


Fig. 5. Performance comparison of the C&CG with modified BD algorithms: System *required* reserve.

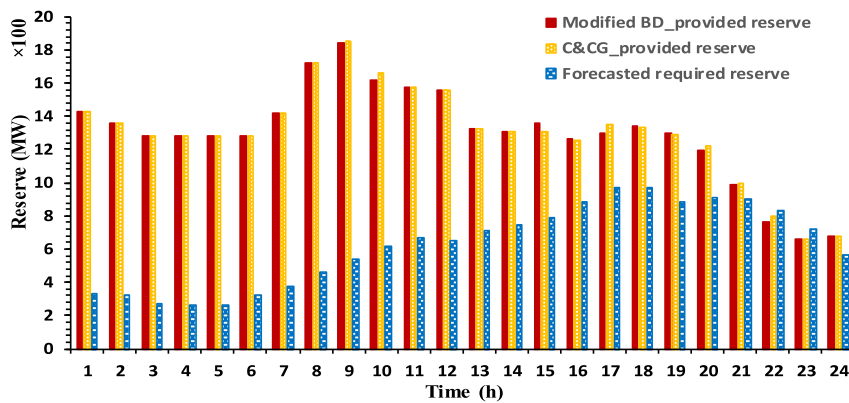


Fig. 6. Performance comparison of the C&CG with modified BD algorithms: *Forecasted* downward reserve and *provided* operating reserve.

hour 22, where the uncertainty interval corresponding to the modified BD is narrower than that when using the C&CG method.

The system’s ability to provide operating reserves can be determined considering the output power of generating units when no uncertainty in generating units’ capacity and ramping capabilities as well as in transmission limits are enforced. The forecasted uncertainty set returns the *required* operating reserve. In case the *provided* reserve is larger than the *required* reserve, the grid will remain secure. Fig. 6 shows the *provided* downward reserve of generating units and the *required* downward reserve

realized from the difference between the *forecasted* upper bound of the uncertainty set and the expected wind generation. It can be seen that the *required* reserve at hours 22 and 23 is higher than the *provided* reserve. Hence, the optimal upper bound value is seen lower than the predefined one and the uncertainty interval is shrunk so as to decrease the amount of *required* reserve.

B. Comparison of Adjustable and Fixed Uncertainty Sets

In order to investigate the impact of adjustable uncertainty set in the two-stage robust SCUC formulation, the benchmarks

TABLE I
SOLUTION COMPARISON OF ROBUST SCUC MODELS

Operation Costs and Corrective Actions		Adjustable US ¹		Fixed US	
		LSBD ²	C&CG	LSBD	C&CG
Base Case	ED cost (k\$)	360.308	359.450	438.987	-
	UC cost (k\$)	2.942	2.943	3.927	-
	LS cost (k\$)	0	0	0	-
	WS cost (k\$)	14.797	10.759	0	-
	Total cost (k\$)	378.048	373.201	442.914	-
Worst Case	ED cost(k\$)	416.290	424.411	521.685	-
	LS action (MW)	0	0	97.99	-
	WS action (MW)	0	0	0	-
	Violation (MW)	0	0	97.99	-

¹US: Uncertainty set.

²LSBD: L-shaped based benders decomposition.

of adjustable [20]–[24] and fixed uncertainty sets [25]–[27] are compared in Table I. In the fixed uncertainty set benchmark, wind power curtailment is taken into consideration in both first and second stages [25]–[27]. In the adjustable uncertainty set benchmark, it is assumed that the wind power production is fixed in the first stage—in the Section V-C, we relax this assumption in the adjustable uncertainty set framework. Additionally, the performance of two solution techniques, the modified BD and C&CG, on the economic dispatch (ED), unit commitment (UC), load shedding (LS), and wind spillage (WS) costs is tabulated.

The superiority of the proposed modified BD and C&CG methods on security violations and redispatch cost is also demonstrated for the worst-case uncertainty realization. Since the convergence speed of the BD algorithm is much slower than that in the proposed modified BD, only the performance of the modified BD and C&CG solution techniques is compared. It is observed that the C&CG approach yields no feasible solution for the robust SCUC problem with a fixed uncertainty set. This is because the worst-case flexibility requirement of a predefined uncertainty set is beyond the flexibility capacity of the system generating units, and consequently, the grid cannot effectively deal with the worst-case wind power realization. Utilizing the suggested C&CG technique, the embedded cuts with no slack variables at each iteration lead to the modified output power of system generating units such that the power balance and transmission line constraints are satisfied even for the worst-case wind realizations. In other words, new cuts causing security violations in the worst-case wind scenarios would be avoided. In the case where the generating units lack sufficient flexibility capacity, security violation cannot be avoided for the worst-case wind deviation. Therefore, the C&CG approach yields no feasible solution. In response, the proposed modified BD algorithm adds some cuts that change the generation schedules such that the worst security violation decreases at each iteration until it converges to a minimum. Even with larger uncertainty intervals, the modified BD still performs efficiently. As can be observed from Table I, in the case of fixed uncertainty sets, the modified BD converges to an optimal schedule with a total violation of

TABLE II
SOLUTION OF ADJUSTABLE PENETRATION RATE TECHNIQUE

Solution Method	ED cost	UC cost	WS cost	RD ¹ cost
C&CG (k\$)	361.973	2.834	16.147	417.501
Modified BD (k\$)	360.779	2.942	17.579	406.273

¹RD: Redispatch.

97.99 MW, which is taken as a measure of flexibility inadequacy. In case of an insufficient flexibility capacity, the C&CG approach will have a feasible solution, only if the uncertainty set is taken into account in the master problem as a variable so that the uncertainty interval shrinks. Comparing the performance of the modified BD algorithm in the case of fixed and variable uncertainty sets, it is observed that a variable uncertainty set in the master problem yields more economical solutions in all studied scenarios. Although reducing the uncertainty interval results in the wind spillage cost in an ex-ante manner, the total operation cost is lower while the system security is ensured. The results also revealed the existence of wind spillage rather than the load shedding mainly due to a higher penalty of the latter.

C. Comparison of Adjustable Uncertainty Set and Adjustable Stochastic Production

The proposed assessment approach based on two-stage robust SCUC with adjustable penetration of wind farms was applied to the test system and the results were numerically compared. The solution techniques, C&CG and the modified BD, are applied and the results are outlined in Table II. Comparison of the results in Tables I and II reveals that although the base-case operation cost considering the adjustable production is higher than that using the variable uncertainty approach, the sum of the base-case and the worst-case (second stage) costs is lower in the proposed adjustable production approach due to its lower recourse cost (RD cost). This is due to the fact that in the former, the wind farms' production is inactivated to immunize the system

TABLE III
OPTIMAL WIND GENERATION PENETRATION AT DIFFERENT HOURS

Solution Method	t=17	t=18	t=22	t=23	Other hours
C&CG (%)	94.94	97.36	97.74	99.08	100
Modified BD (%)	98.01	98.94	98.42	98.78	100

security. As a result, the operation cost in the base-case scenario has increased due to a lower contribution of wind and the intensified net-load. On the other hand, the recourse cost in the proposed approach decreases as the net-load uncertainty and system flexibility cost decrease.

It is worth mentioning that in the first stage of the proposed adjustable penetration approach, load shedding cost never happens. It can also be observed that with penetration variation when using the C&CG approach, the UC cost is found lower compared with the UC cost obtained from the variable uncertainty set technique. The reason lies in the fact that reducing the penetration of wind farms will decrease the variability in the net-load. Another observation from Tables I and II is that in both the adjustable uncertainty set and adjustable penetration techniques, the second-stage economic dispatch (ED) cost (RD cost), when the modified BD approach is applied, is observed lower than that when the C&CG method is approached. The reason is that the first-stage wind spillage in the former is higher, which leads to a narrower uncertainty interval.

Table III presents the optimal utilization percentage of the expected wind generation (i.e., the optimal penetration). It can be observed that at hours 17, 18, 22, and 23, the total penetration of wind farms is less than 100% and wind curtailment occurs consequently. With the higher uncertainty intervals at hours 17 and 18 due to higher wind generation, the wind power penetration is obtained lower than 100% in order to shrink the uncertainty interval such that the system can have the ability to effectively react to the uncertainty. Lower penetration at hours 22 and 23 is due to the fact that the net-load at these hours is at the minimum. Consequently, the generating units are dispatched at lower power outputs and their downward ramping abilities decreased. Thus, with the reduction in wind penetration, the net-load has increased. Accordingly, the ability of generating units downward ramping will increase.

D. Additional Analyses

For further comparison of the proposed model versus the state-of-the-art benchmark models, we explore the performance of the proposed model using an after-the-fact analysis. To do so, for each wind farm, 1000 wind trajectories each including the production of that farm over 24 h are generated with respect to the uncertainty boundaries. We assume that the uncertainty follows a uniform distribution. Considering the commitment and dispatch of generating units achieved in the first stage of the robust UC model, real-time dispatch simulation is carried out with the generated wind power trajectories. Table IV depicts the promising after-the-fact performance of the proposed adjustable uncertainty set model compared with the fixed uncertainty set benchmark in terms of mean, standard deviation, and CVaR (5%) of the redispatch cost. Additionally, for further comparison of

TABLE IV
AFTER-THE-FACT RESULTS: THE REDISPATCH COST IN TERMS OF MEAN, STANDARD DEVIATION, AND CVaR (5%)

Model and Solution Method		Re-dispatch cost (k\$)		
		Mean	Standard deviation	CVaR (5%)
Proposed Adjustable Penetration Model	C&CG	115.49	13.71	76.61
	Modified BD	100.27	12.41	66.27
Fixed Uncertainty Set Benchmark	Modified BD	161.81	20.5	90.60

TABLE V
AFTER-THE-FACT RESULTS: THE REDISPATCH COST FOR DIFFERENT SCENARIOS OF LOAD LEVEL

Re-dispatch Cost (k\$)	Load Level		
	0.9	1	1.1
Proposed Adjustable Penetration Model	79.07	115.49	127.71
Fixed Uncertainty Set Benchmark	90.16	161.81	164.61

the proposed model versus the fixed uncertainty set benchmark, we consider three scenarios representing multiple days. Under these three scenarios, the load level is assumed to be 0.9, 1, and $1.1 \times$ of the load level given in [29] with the same profile pattern. Table V depicts a stronger after-the-fact performance of the proposed model.

VI. CONCLUSION

In this article, a novel mathematical model centered on the adjustable production of stochastic producers was presented to assess the power grid operational flexibility. The suggested approach enabled the assessment of the worst recourse cost under various uncertainty scenarios, through which the effect of uncertainty cost of stochastic producers can be modeled in the flexibility assessments. In order to evaluate the economically optimal stochastic production, the penetration of stochastic producers was adjusted using an RO approach to make a balance between the UC and dispatch cost in the base-case scenario and the recourse cost in the worst-case realizations. The efficiency of the proposed approach was compared with the other state-of-the-art adjustable and fixed uncertainty set techniques. It was concluded that the proposed technique outperformed the conventional methods from both technical and economical perspectives. This article also suggested a modified BD algorithm based on the L-shaped technique to deal with high computational burdens and feasibility challenges associated with the conventional BD and C&CG algorithms. The proposed modified BD method outperformed the C&CG approach in cases where the uncertainty set was fixed and the redispatch flexibility was not sufficient.

The performance of the proposed assessment techniques was numerically investigated and verified.

ACKNOWLEDGMENT

Any opinions, findings, and conclusions or recommendations expressed in this article are those of the authors and do not necessarily reflect the views of the National Science Foundation.

REFERENCES

- [1] P. de Martini, K. M. Chandy, and N. A. Fromer, "Grid 2020: Towards a policy of renewable and distributed energy resources," Resnick Institute, Pasadena, CA, USA, 2012.
- [2] J. P. Chaves-Avila, K. Wurzburg, T. Gomez, and P. Linares, "The green impact: How renewable sources are changing EU electricity prices," *IEEE Power Energy Mag.*, vol. 13, no. 4, pp. 29–40, Jul./Aug. 2015.
- [3] J. Cochran *et al.*, *Flexibility in 21st Century Power Systems*. Golden, CO, USA.: Nat. Renewable Energy Lab., 2014.
- [4] N. Menemenlis, M. Huneault, and A. Robitaille, "Thoughts on power system flexibility quantification for the short-term horizon," in *Proc. IEEE Power Energy Soc. General Meeting*, Detroit, MI, USA, 2011, pp. 1–8.
- [5] F. D. Galiana, F. Bouffard, J. M. Arroyo, and J. F. Restrepo, "Scheduling and pricing of coupled energy and primary, secondary, and tertiary reserves," *Proc. IEEE*, vol. 93, no. 11, pp. 1970–1983, Nov. 2005.
- [6] Y. G. Rebours, D. S. Kirschen, M. Trotignon, and S. Rossignol, "A survey of frequency and voltage control ancillary services—Part I: Technical features," *IEEE Trans. Power Syst.*, vol. 22, no. 1, pp. 350–357, Feb. 2007.
- [7] "Supporting document for the network code on load-frequency control and reserves," Tech. Rep., Eur. Netw. Transmiss. Syst. Operators Elect., Brussels, Belgium, 2013.
- [8] H. Nosair and F. Bouffard, "Flexibility envelopes for power system operational planning," *IEEE Trans. Sustain. Energy*, vol. 6, no. 3, pp. 800–809, Jul. 2015.
- [9] Y. V. Makarov, C. Loutan, and P. de Mello, "Operational impacts of wind generation on California power systems," *IEEE Trans. Power Syst.*, vol. 24, no. 2, pp. 1039–1050, May 2009.
- [10] Y. Dvorkin, H. Pandžić, M. A. Ortega-Vazquez, and D. S. Kirschen, "A hybrid stochastic/interval approach to transmission-constrained unit commitment," *IEEE Trans. Power Syst.*, vol. 30, no. 2, pp. 621–631, Mar. 2015.
- [11] F. Bouffard and F. D. Galiana, "Stochastic security for operations planning with significant wind power generation," *IEEE Trans. Power Syst.*, vol. 23, no. 2, pp. 306–316, May 2008.
- [12] S. M. Chan, D. C. Powell, M. Yoshimura, and D. H. Curtice, "Operations requirements of utilities with wind power generation," *IEEE Trans. Power App. Syst.*, vol. PAS-102, no. 9, pp. 2850–2860, Sep. 1983.
- [13] J. Kiviluoma *et al.*, "Short-term energy balancing with increasing levels of wind energy," *IEEE Trans. Sustain. Energy*, vol. 3, no. 4, pp. 769–776, Oct. 2012.
- [14] P. Carpentier, G. Cohen, J.-C. Culioli, and A. Renaud, "Stochastic optimization of unit commitment: A new decomposition framework," *IEEE Trans. Power Syst.*, vol. 11, no. 2, pp. 1067–1073, May 1996.
- [15] L. Wu, M. Shahidehpour, and T. Li, "Stochastic security-constrained unit commitment," *IEEE Trans. Power Syst.*, vol. 22, no. 2, pp. 800–811, May 2007.
- [16] D. Bertsimas, E. Litvinov, X. A. Sun, J. Zhao, and T. Zheng, "Adaptive robust optimization for the security constrained unit commitment problem," *IEEE Trans. Power Syst.*, vol. 28, no. 1, pp. 52–63, Feb. 2013.
- [17] R. Jiang, J. Wang, and Y. Guan, "Robust unit commitment with wind power and pumped storage hydro," *IEEE Trans. Power Syst.*, vol. 27, no. 2, pp. 800–810, May 2012.
- [18] C. Zhao, J. Wang, J.-P. Watson, and Y. Guan, "Multi-stage robust unit commitment considering wind and demand response uncertainties," *IEEE Trans. Power Syst.*, vol. 28, no. 3, pp. 2708–2717, Aug. 2013.
- [19] A. A. Thatte and L. Xie, "A metric and market construct of inter-temporal flexibility in time-coupled economic dispatch," *IEEE Trans. Power Syst.*, vol. 31, no. 5, pp. 3437–3446, Sep. 2016.
- [20] Z. Qin, Y. Hou, S. Lei, and F. Liu, "Quantification of intra-hour security-constrained flexibility region," *IEEE Trans. Sustain. Energy*, vol. 8, no. 2, pp. 671–684, Apr. 2017.
- [21] J. Zhao, T. Zheng, and E. Litvinov, "A unified framework for defining and measuring flexibility in power systems," *IEEE Trans. Power Syst.*, vol. 31, no. 1, pp. 339–347, Jan. 2016.
- [22] J. Zhao, T. Zheng, and E. Litvinov, "Variable resource dispatch through do-not-exceed limit," *IEEE Trans. Power Syst.*, vol. 30, no. 2, pp. 820–828, Mar. 2015.
- [23] C. Shao, X. Wang, M. Shahidehpour, X. Wang, and B. Wang, "Security-constrained unit commitment with flexible uncertainty set for variable wind power," *IEEE Trans. Sustain. Energy*, vol. 8, no. 3, pp. 1237–1246, Jul. 2017.
- [24] C. Wang *et al.*, "Robust risk-constrained unit commitment with large-scale wind generation: An adjustable uncertainty set approach," *IEEE Trans. Power Syst.*, vol. 32, no. 1, pp. 723–733, Jan. 2017.
- [25] Z. Zhang, Y. Chen, X. Liu, and W. Wang, "Two-stage robust security-constrained unit commitment model considering time autocorrelation of wind/load prediction error and outage contingency probability of units," *IEEE Access*, vol. 7, pp. 25398–25408, 2019.
- [26] C. Dai, L. Wu, and H. Wu, "A multi-band uncertainty set based robust SCUC with spatial and temporal budget constraints," *IEEE Trans. Power Syst.*, vol. 31, no. 6, pp. 4988–5000, Nov. 2016.
- [27] B. Hu, L. Wu, and M. Marwali, "On the robust solution to SCUC with load and wind uncertainty correlations," *IEEE Trans. Power Syst.*, vol. 29, no. 6, pp. 2952–2964, Nov. 2014.
- [28] C. Grigg *et al.*, "The IEEE reliability test system-1996. A report prepared by the reliability test system task force of the application of probability methods subcommittee," *IEEE Trans. Power Syst.*, vol. 14, no. 3, pp. 1010–1020, Aug. 1999.
- [29] H. Pandzic *et al.*, "Unit commitment under uncertainty - GAMS models, library of the renewable energy analysis lab (REAL)," Univ. Washington, Seattle, WA, USA. [Online]. Available: http://www.ee.washington.edu/research/real/gams_code.html



Farzaneh Pourahmadi (Student Member, IEEE) received the M.S. and Ph.D. degrees in electrical engineering from the Sharif University of Technology, Tehran, Iran, in 2014 and 2019, respectively.

From June 2018 to June 2019, she was a Visiting Researcher with the Department of Electrical Engineering, Technical University of Denmark, Lyngby, Denmark. Her research interests include power system planning and operation, as well as optimization and its application to power systems.



Seyed Hamid Hosseini (Member, IEEE) received the Ph.D. degree in electrical engineering from the Iowa State University, Ames, IA, USA, in 1988.

Since 1988, he has been with the Department of Electrical Engineering, Sharif University of Technology, Tehran, Iran, where currently he is a Full Professor. His current research interests include power system operation, optimization, planning, and renewable energy.



Payman Dehghanian (Member, IEEE) received the B.Sc., degree from the University of Tehran, Tehran, Iran, in 2009, M.Sc. degree from the Sharif University of Technology, Tehran, Iran, in 2011, and the Ph. D. degree from Texas A&M University, College Station, Texas, USA, in 2017, respectively all in electrical engineering.

He is an Assistant Professor with the Department of Electrical and Computer Engineering, George Washington University, Washington, DC, USA. His research interests include power system online situational awareness, real-time decision making, power system reliability and resiliency, asset management, and smart electricity grid applications.

Dr. Dehghanian was a recipient of the 2013 IEEE Iran Section Best M.Sc. Thesis Award in electrical engineering, the 2014 and 2015 IEEE Region 5 Outstanding Professional Achievement Awards, and the 2015 IEEE-HKN Outstanding Young Professional Award.



Ekundayo Shittu (Member, IEEE) received the B.Eng. degree in electrical engineering from the University of Ilorin, Ilorin, Nigeria, in 1998, the M.S. degree in industrial engineering from The American University in Cairo, Cairo, Egypt, in 2004, and the Ph.D. degree in industrial engineering and operations research from the University of Massachusetts Amherst, Amherst, MA, USA, in 2009.

He is an Assistant Professor with the Department of Engineering Management and Systems Engineering, George Washington University, Washington, DC, USA. He was a Lead Author of chapter 2, “Integrated Risk and Uncertainty Assessment of Climate Change Response Policies,” of Working Group III to the 5th Assessment Report (AR5) of the Intergovernmental Panel on Climate Change. His current research agenda in the arena of technology management and the economics of renewable energy focuses on the interplay among public policy, competition, and energy technology investments. His research also studies the strategic interaction between firms’ technology stocks and the external environment through the lenses of transaction cost economics and resource-based view.

Dr. Shittu is a member of the Institute for Operations Research and the Management Sciences, Production and Operations Management Society, International Association for Energy Economics, Strategic Management Society, and the International Council on Systems Engineering. Some of the journals he reviews include the IEEE TRANSACTIONS IN ENGINEERING MANAGEMENT, IEEE TRANSACTIONS IN POWER SYSTEMS, *Production and Operations Management*, *Renewable and Sustainable Energy Reviews*, *Applied Energy*, *Energy Economics*, *Naval Research Logistics*, *Vaccines*, *Risk Analysis*, *Systems Engineering*, and *Climate Policy*. His research has been funded by multiple awards from the National Science Foundation, Department of Energy, Alfred P. Sloan Foundation, Duke Energy Renewables, etc. He has reviewed *Practical Management Science* 4th–6th editions by Wayne Winston and Christian Albright. He coauthored *Renewable Energy: International Perspectives on Sustainability* (Springer).



Mahmud Fotuhi-Firuzabad (Fellow, IEEE) received the B.Sc. degree from the Sharif University of Technology, Tehran, Iran, the M.Sc. degree from Tehran University, Tehran, Iran, in 1986 and 1989, respectively, both in electrical engineering and the M.Sc. and Ph.D. degrees in electrical engineering from the University of Saskatchewan, Saskatoon, SK, Canada, in 1993 and 1997, respectively.

He is a Professor of the Department of Electrical Engineering and the President of the Sharif University of Technology, Tehran, Iran. He is a member of the Center of Excellence in Power System Control and Management with the same department. His research interests include power system reliability, distributed renewable generation, demand response, and smart grids.

Dr. Fotuhi-Firuzabad was a recipient of several national and international awards including the World Intellectual Property Organization Award for the Outstanding Inventor, in 2003, and PMAPS International Society Merit Award for the contributions of probabilistic methods applied to power systems in 2016. He is a Visiting Professor with Aalto University, Espoo, Finland. He serves as the Editor-in-Chief for the IEEE POWER ENGINEERING LETTERS.